Stoichiometry of Expressed KCNQ2/KCNQ3 Potassium Channels and Subunit Composition of Native Ganglionic M Channels Deduced from Block by Tetraethylammonium

Jennifer K. Hadley,[1] Gayle M. Passmore,[1] Lucine Tatulian,[1] Mona Al-Qatari,[1] Fei Ye,[2] Alan D. Wickenden,[2] and David A. Brown[1]

[1]Department of Pharmacology, University College London, London WC1E 6BT, United Kingdom, and [2]Icagen Inc., Durham, North Carolina 27703

KCNQ2 and KCNQ3 potassium-channel subunits can form both homomeric and heteromeric channels; the latter are thought to constitute native ganglionic M channels. We have tried to deduce the stoichiometric contributions of KCNQ2 and KCNQ3 subunits to currents generated by the coexpression of KCNQ2 and KCNQ3 cDNA plasmids in Chinese hamster ovary (CHO) cells, and to native M currents in dissociated rat superior cervical ganglion (SCG) neurons, by comparing the block of these currents produced by tetraethylammonium (TEA) with the block of currents generated by a tandem KCNQ3/2 construct. TEA concentration–inhibition curves against coexpressed KCNQ2 plus KCNQ3 currents, and against native M currents in SCG neurons from 6-week-old [postnatal day 45 (P45)] rats, were indistinguishable from those for the expressed tandem construct, and fully accorded with a 1:1 stoichiometry. Inhibition curves in neurons from younger (P17) rats could be better fitted assuming an additional small proportion of current carried by KCNQ2 homomultimers. Single-cell PCR yielded signals for KCNQ2, KCNQ3, and KCNQ5 mRNAs in all SCG neurons tested from both P17 and P45 rats. Quantitative PCR of whole-ganglion mRNA revealed stable levels of KCNQ2 and KCNQ5 mRNA between P7 and P45, but excess and incrementing levels of KCNQ3 mRNA. Increasing levels of KCNQ3 protein between P17 and P45 were confirmed by immunocytochemistry. We conclude that coexpressed KCNQ2 plus KCNQ3 cDNAs generate channels with 1:1 (KCNQ2:KCNQ3) stoichiometry in CHO cells and that native M channels in SCG neurons adopt the same conformation during development, assisted by the increased expression of KCNQ3 mRNA and protein.

Key words: **TEA; KCNQ channels; M current; Chinese hamster ovary (CHO) cell; sympathetic neurons; stoichiometry; concatenated channel subunits**

Introduction

KCNQ channels are a family of five voltage-gated K^+ channel subunits, four of which (KCNQ2–5) are present in the nervous system (Jentsch, 2000). Although they are capable of forming homomeric channels, KCNQ3 subunits can also form heteromeric (presumed tetrameric) channels by coassembly with KCNQ2, 4, or 5 subunits (Jentsch, 2000). Coassembled KCNQ2 and KCNQ3 subunits probably form the native M channel in rat sympathetic neurons (Wang et al., 1998; Shapiro et al., 2000; Selyanko et al., 2001). This channel generates a species of low-threshold, noninactivating K^+ current (the M current) that regulates the excitability of sympathetic and some central neurons and that is inhibited by stimulating muscarinic acetylcholine receptors and some related G-protein-coupled receptors (Brown and Adams, 1980; Brown, 1988; Marrion, 1997).

Coexpressed KCNQ2 and KCNQ3 subunits show much higher surface expression (Schwake et al., 2000) and usually generate larger currents (Wang et al., 1998; Yang et al., 1998; Selyanko et al., 2001) than when either is expressed alone. Immunoprecipitation studies also show that these two subunits are normally associated in the brain *in situ* (Cooper et al., 2000). However, heteromerization is not obligatory for functional channel expression. Furthermore, neither the precise stoichiometry of expressed KCNQ2 plus KCNQ3 combinations nor that of the subunit contributions to the native M channels are yet clear.

The subunit stoichiometry of some other heteromeric K^+ channels has been assessed by comparing the blocking action of a compound with a widely differing affinity for the two subunits (such as tetraethylammonium, TEA) on homomeric and heteromeric currents (Christie et al., 1990; Heginbotham and MacKinnon, 1992; Kavanaugh et al., 1992; Liman et al., 1992). This approach can also be used for KCNQ2/KCNQ3 channels because homomeric KCNQ2 channels have a much higher (>100-fold) affinity for TEA than homomeric KCNQ3 channels by virtue of a tyrosine group in the upper pore vestibule, which is replaced by a threonine in KCNQ3 (Hadley et al., 2000; cf. MacKinnon and Yellen, 1990; Kavanaugh et al., 1991). However, previous measurements of TEA inhibition of coexpressed KCNQ2 plus KCNQ3 currents have yielded somewhat conflicting results.

Received Jan. 23, 2003; revised March 17, 2003; accepted March 25, 2003.

This work was supported by United Kingdom Medical Research Council Grant PG 7909913, Wellcome Trust Grant 038170, and European Union Grant QL-G3-CT-1999-00827. We thank Dr. D. McKinnon (State University of New York at Stony Brook, Stony Brook, NY) for the human KCNQ2 cDNA, Dr. S. A. Burbidge (Systems Research, GlaxoSmithKline, Stevenage, Hertfordshire, UK) for the gift of anti-KCNQ3 antiserum, Dr. Alvaro Villarroel (Cajal Institute, Madrid, Spain) for the gift of anti-KCNQ5 antiserum, Dr. Fe Abogadie for growing the plasmids, and Tahiba Rafiq and Joanne Reilly for culture of superior cervical ganglia.

Correspondence should be addressed to D. A. Brown, Department of Pharmacology, University College London, Gower Street, London WC1E 6BT, UK. E-mail: d.a.brown@ucl.ac.uk.

J. K. Hadley's present address: Department of Physiology, Royal Free Hospital School of Medicine, Rowland Hill Street, London NW3 2PF, UK.

M. Al-Qatari's present address: Institute of Child Health, University College London, 30 Guilford Street, London WC1N 1EH, UK.

 0270-6474/03/235012-08$15.00/0

Thus, Wang et al. (1998) (in oocytes) and Hadley et al. (2000) [in Chinese hamster ovary (CHO) cells] obtained monotonic concentration–inhibition curves with a near-unity (0.8) Hill slope, as if the currents were generated predominantly by channels composed of the two subunits in a single (possibly 1:1) stoichiometry. However, Shapiro et al. (2000; mammalian tsA cells) obtained a shallow (but incomplete) concentration–inhibition curve more compatible with a random subunit assembly.

The interpretation of such experiments can be facilitated by comparing the inhibition of currents generated by coexpressed single subunits with the inhibition of currents generated by tandem cDNA constructs (Kavanaugh et al., 1992; Liman et al., 1992). Hence, we have compared the effects of TEA on currents generated in CHO cells by coexpression of cDNAs for separate human KCNQ2 and KCNQ3 subunits with its effect on currents generated by expressing a human KCNQ3/2 tandem construct (Wickenden et al., 2000). We have also compared the properties of these *in vitro* human KCNQ2/3 M currents with those of native M currents in dissociated rat sympathetic neurons, and have matched the results against the expression of KCNQ subunits as determined by single-cell and whole-ganglion PCR and by immunocytochemistry.

Materials and Methods

DNA plasmids. Human KCNQ2 cDNA (as studied by Wang et al., 1998) was provided by Dr. D. McKinnon (State University of New York at Stony Brook, Stony Brook, NY); the human KCNQ3 and KCNQ3/2 tandem sequences were generated at Icagen, Inc. (Durham, NC). The KCNQ2 cDNA is not identical to the KCNQ2 portion of the dimeric construct, but sequence differences are confined to the C terminal. Principally, a 10 aa stretch (corresponding to exon 8 in Pan et al., 2001) is present, and a later stretch of 11 aa (the second half of exon 11) is absent in D. McKinnon's KCNQ2 compared with the Icagen sequence. These are not expected to affect the expression or kinetics appreciably (Pan et al., 2001), and they are remote from the TEA-sensitive pore region.

Cell culture and transfection. Culture and transfection of CHO cells was as described by Selyanko et al. (1999). CHO cells were grown at 37°C and in 5% CO_2 in α-MEM supplemented with 10% fetal calf serum, 1% L-glutamine, and 1% penicillin/streptomycin. For recording, cells were plated in 35 mm plastic dishes and transfected 1–2 d after plating using LipofectAmine Plus (Invitrogen, Gaithersburg, MD) as suggested by the manufacturer. Plasmids (driven by a cytomegalovirus promoter) containing cDNAs for KCNQ channels and cDNA for CD8 as a marker were cotransfected at a channel:marker ratio of 10:1. Cotransfections of KCNQ2 with KCNQ3 were in a 1:1 weight ratio. Cells for patch clamping were identified using CD8-binding Dynabeads (Dynal, Great Neck, NY) 1 d after transfection. Superior cervical ganglion (SCG) neurons were prepared as described previously (Owen et al., 1990) from 17-d-old (P17) or 6-week-old (P45) Sprague Dawley rats, and used after 1 d in culture.

Recording. The perfusing solution contained the following (in mM): 144 NaCl, 2.5 KCl, 2 $CaCl_2$, 0.5 $MgCl_2$, 5 HEPES, and 10 glucose, plus Tris base to pH 7.4. The pipette solution contained the following (in mM): 90 K acetate, 20 KCl, 40 HEPES, 3 $MgCl_2$, 3 EGTA, 1 $CaCl_2$, and NaOH to pH 7.4. These solutions give rise to a junction potential of −7 mV, left uncorrected here for consistency with other publications from this laboratory. Amphotericin B was used to perforate the patch (Rae et al., 1991). TEA was applied cumulatively in doses of 0.03–30 mM, using 0.2 and 2 M aqueous TEA stock solutions added to the perfusion reservoir. All experiments were done at room temperature (22–26°C).

Data acquisition and initial analysis used pClamp8 software (Axon Instruments, Foster City, CA). Currents were recorded using an Axopatch 200A (or 200B) patch-clamp amplifier (Axon Instruments), filtered at 1 kHz, and digitized at 1–4 kHz. When possible, capacity transients were neutralized and series resistance compensated up to 90%. Current–voltage relationships and time constants were obtained using deactivating steps from a holding potential of −20 mV. For TEA inhibition, 1 sec steps to −50 mV were applied from a holding potential of −20 mV, and the total relaxation amplitude at −50 mV was measured for a single control trace and a single trace for each dose of TEA.

Analysis. Data were normalized in Excel 97 (Microsoft, Seattle, WA) and plotted in Origin (version 5.0, Microcal Software). TEA concentration–inhibition curves were initially fitted with the Hill equation:

$$y/y_{max} = 1/(1 + (x/x_0)^p), \quad (1)$$

where y is the relaxation amplitude; y_{max} is full inhibition; x is the concentration of the blocker; x_0 is the IC_{50} (the concentration at which $y/y_{max} = 0.5$); and p is the power (equivalent to the Hill slope, n_H). For the two-component fit to TEA inhibition of the rat sympathetic M-current, a modified equation was applied in Origin. This had the form:

$$y/y_{max} = q(1 + x/x_0) + (1 - q)/(1 + x/x_1), \quad (2)$$

where x_0 and x_1 are the IC_{50}s for two channel populations with proportional contributions of q and $(1 - q)$, respectively (other definitions as above). The factor p was not included because we assumed the presence of separate channel populations each with a Hill slope of unity. In all cases, y_{max} was taken to be 100%, even if full inhibition was not obtained at the highest TEA concentration used.

To avoid misleading slope values caused by data averaging, inhibition curves were fitted separately for every cell, before averaging IC_{50} and slope values. For IC_{50}s, which are log-normally distributed, geometrically/logarithmically based averages are most appropriate. We give here the geometric mean IC_{50} (the nth root of the product of n values) as an easily read equivalent to the arithmetically averaged pIC_{50} (or negative logarithm of the IC_{50} to base 10) for current block. As a trial, a Boltzmann equation was also fitted to inhibition data plotted against log TEA concentrations in Origin (as in Hadley et al., 2000), for individual KCNQ3/KCNQ2-expressing cells. The fitting process yielded log IC_{50} values matching the logarithms of IC_{50}s from the Hill equation fitted to at least three significant digits, so we considered the log transformation of concentrations to be unnecessary for accurate fitting. Hence, all data are expressed as the geometric mean (mM) with 95% confidence limits (CL) in brackets. Statistical analysis was performed in Excel 97 and InStat (GraphPad, version 2.04a; GraphPad Software Inc., San Diego, CA).

Single-cell PCR. The method used here has been adapted from Zawar et al. (1999). Cytosol from single sympathetic neurons was collected into 7.5 μl of recording buffer and eluted into a tube containing 2.5 μl of first-strand buffer (2 mM deoxynucleotide triphosphate, 20 μM oligo-dT_{15}, 40 mM dithiothreitol, and 20 U RNase inhibitor; Roche Products, Hertfordshire, UK). Reverse transcription of mRNA transcripts were initiated by the addition of 100 U Moloney murine leukemia virus reverse transcriptase, RNase H (−) point mutant (Promega, Madison, WI) and by incubation at 37°C for 1 hr. A multiplex PCR protocol was then used to amplify simultaneously cDNA for KCNQ2–5. Primers were designed to be intron-spanning (as deduced from the human KCNQ genes) and were as follows: rat KCNQ2 (rKCNQ2) 2900 sec AGTGCGGATCAGAGTCTC; KCNQ2 3126a GCTCTGATGCTGACTTTGAGGC; rKCNQ3 746 sec CAGCAAAGAACTCATCACCG; rKCNQ3 906a ATGGTGGCCAGTGTGATCAG; rKCNQ4 40 sec CCCTCCAAGCAGCATCTG; rKCNQ4 420a TTGATTCGTCCCAGCATGTCCA; human KCNQ5 (hKCNQ5) 995 sec GGAACCCAGCTGCCAACCTCAT; and hKCNQ5 1101 sec CTTTCTTGGTAGGGCTGCAG.

Multiplex PCR amplification was performed by the addition of 5 U *Taq* polymerase (Promega, Southhampton, UK) in a standard PCR buffer to 10 μl of single-cell reverse transcriptase (RT) product to give a final volume of 70 μl. The primers (10 pmol each) were added in a volume of 30 μl. PCR amplification consisted of 35 cycles of denaturation at 94°C for 30 sec, annealing at 55°C for 30 sec, and elongation at 72°C for 40 sec; followed by elongation for 10 min at 72°C. The products of the multiplex amplification were purified using the High Pure PCR purification kit (Roche). Gene-specific PCRs were then performed on 3 μl of amplified cDNA template. No signals were detected in the absence of template.

Quantitative PCR. Total RNA was extracted from whole ganglia isolated from embryonic day 18 (E18)/E19, P7, P17, and P45 rats and additionally treated with DNase I. First-strand cDNA was synthesized from purified RNA using Superscript II reverse transcriptase and oligo-dT (Invitrogen). Taqman real-time quantitative RT-PCR was performed using ABI Prism 7900 (PE Applied Biosystems, Foster City, CA). Taqman primer and probe sets for KCNQ2–5 targets were designed based on rat (KCNQ2, GenBank accession number AF087453; KCNQ3, AF091247; KCNQ4, AF249748) or human (KCNQ5, AF202977) sequences. They were as follows: KCNQ2-forward: 5′-GCGACACGTCCATCTCCAT-3′ (2412–2431); KCNQ2-reverse: 5′-GGAGATACTGAAACCGCTAAAGGA-3′ (2486–2462); KCNQ2-probe: 5′-CGGTGGACCACGAGGAGCTGGAG-3′ (2439–2459); KCNQ3-forward: 5′-ACACACCACTGTCCCTCATGTC-3′ (2234–2256); KCNQ3-reverse: 5′-TCTGTCTTGGGAGATGCTGAAG-3′ (2414–2392); KCNQ3-probe: 5′-TCAACCACGAGGAACTGGAACGGTCT-3′ (2813–2835); KCNQ4-forward: 5′-CTGTGAAGACGGTCATCCGTTCT-3′ (275–298); KCNQ4-reverse: 5′-AGCGTCTCCTTGAATTTCCTT-3′ (348–327); KCNQ4-probe: 5′-CAGGATTCTGAAGTTCCTGGTAGCC-3′ (300–325); KCNQ5-forward: 5′-GCACCGACCTCCTCATCAGT-3′ (2452–2474); KCNQ5-reverse: 5′-TCTCGAGGCAGCCAAGATTT-3′ (2528–2509); and KCNQ5-probe: 5′-TTTGGATTCTCTCCACTTGGGATA-3′ (2475–2499).

Primers and probe for endogenous control glyceraldehyde-3-phosphate dehydrogenase (GAPDH) were obtained from PE Applied Biosystems. The PCRs were performed using Taqman universal PCR master mix (PE Applied Biosystems) with 300 nM primers and 200 nM fluorogenic probe. For the signal detection, ABI Prism 7900 sequence detector was programmed to an initial step of 2 min at 50°C and 10 min at 95°C, followed by 40 thermal cycles of 15 sec at 95°C and 1 min at 60°C. Each measurement was performed in duplicate and repeated. Relative standard curve method (Gibson et al., 1996; Heid et al., 1996) was used to determine the KCNQ2–5 transcript levels in rat SCG. Standard curves for KCNQ2–5 targets and endogenous control GAPDH were constructed using serial dilutions of cDNA fragments cloned from rat dorsal root ganglion. Differences in the total amount of RNA present in each sample were normalized with GAPDH. The final result of the expression level is presented as a percentage of GAPDH.

Immunocytochemistry. Immunocytochemistry for KCNQ subunits was undertaken on neurons dissociated from sympathetic ganglia isolated from 17-d-old and 6-week-old rats (P17 and P45) and cultured on laminin-coated glass coverslips for 1 d. Cultures were rinsed three times with PBS for 5 min, then fixed with freshly prepared 4% paraformaldehyde in PBS for 30 min at room temperature. They were then quenched twice with 0.37% glycine/0.27% ammonium chloride in PBS for 10 min, followed by PBS rinses. After permeabilization with 0.1% Triton X-100 in PBS for 15 min, a blocking solution of 2% bovine serum albumin (BSA) plus 2% fetal calf serum in PBS was applied for 60 min. After rinsing three times with 1% BSA in PBS, the cells were incubated overnight at 4°C with the relevant antibodies diluted in 1% BSA in PBS. The primary antibodies used were goat anti-KCNQ2 (1:100; Santa Cruz Biotechnology, Santa Cruz, CA),rabbit anti-KCNQ3 (1:100; provided by S.A. Burbidge, GlaxoSmithKline, Stevenage, UK), and rabbit anti-KCNQ5 (1:500; provided by A. Villarroel, Cajal Institute, Madrid, Spain). After washing six times for 5 min with 1% BSA in PBS, cells were incubated with tetramethylrhodamine isothiocyanate- or FITC-coupled secondary antibodies (1:1000; Molecular Probes, Eugene, OR). After six additional washes with 1% BSA in PBS and a final wash with PBS alone, coverslips were mounted on ethanol-cleaned slides using a fluorescence mounting medium (DakoCarpinteria, CA) and visualized with a Leica (Nussloch, Germany) confocal microscope. Images were obtained using 40× or 100× objectives with sequential acquisition settings at 1024 × 10^{24} pixel resolution. Specificity was checked by preabsorbing the antibodies with the relevant immunogenic peptide (20:1 excess).

Drugs and chemicals. TEA was from Lancaster Synthesis (Windham, NH). All other chemicals were obtained from Sigma (St. Louis, MO) or BDH Chemicals (Poole, UK).

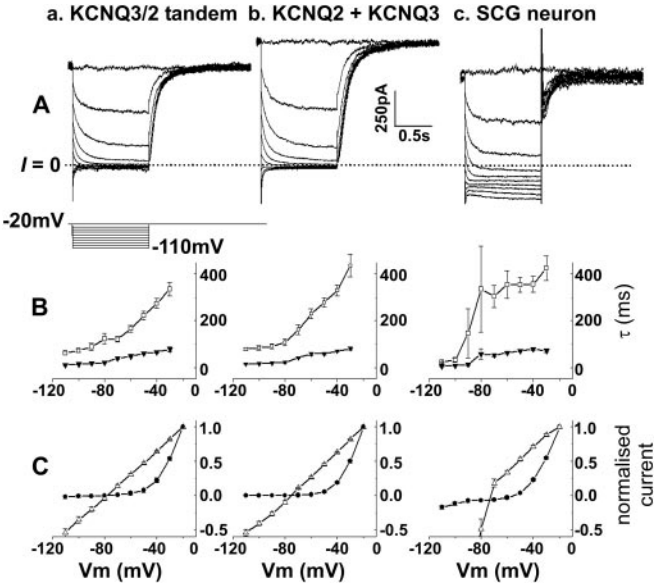

Figure 1. Similar kinetics of currents generated by expressed KCNQ3/2 tandem cDNA (*a*) and coexpressed KCNQ2 and KCNQ3 cDNAs in CHO cells (*b*), and native M/KCNQ currents (*c*) in dissociated P17 rat SCG neurons. *A*, Typical currents. Cells were held at −20 mV to preactivate currents. Records show deactivation currents induced by 1 sec hyperpolarizing steps in increments of −10 mV at 20 sec intervals. *B*, Mean fast (filled triangles) and slow (open squares) deactivation time constants (τ) plotted against deactivation potential. Number of cells: 11 (*a*), 12 (*b*), and 17 (*c*). *C*, Mean instantaneous (open triangles) and steady-state (filled circles) current–voltage relationships. Number of cells as in *B*.

Results

Kinetics of expressed KCNQ2/KCNQ3 currents and native M currents

The concatenated KCNQ3/2 sequence, when expressed in CHO cells and recorded 1 d after transfection, produced substantial currents, often ≥1 nA at −20 mV, similar in size and shape to those resulting from the cotransfection of equal amounts of KCNQ2 and KCNQ3 cDNA.

Figure 1 compares deactivation tail currents generated by hyperpolarizing steps from a holding potential (V_m) of −20 mV for concatenated and coexpressed human KCNQ2/KCNQ3 channel subunits, and for a rat SCG neuron. Also shown are the averaged deactivation time constants and normalized current–voltage curves. Current deactivation was best fitted with two exponential components, as reported previously for tandem KCNQ3/2 currents (Wickenden et al., 2000) and for coexpressed KCNQ2 plus KCNQ3 currents (Pan et al., 2001). The current–voltage curves and deactivation kinetics for the coexpressed KCNQ2 and KCNQ3 subunits were virtually indistinguishable from those for the tandem KCNQ3/2 construct.

SCG M currents were generally smaller, difficult to compensate, and contaminated by a hyperpolarization-activated current (Lamas, 1998), making kinetic data harder to measure consistently. Nevertheless, their kinetics were also very similar to those of the expressed KCNQ channels (notwithstanding the species difference): note particularly the comparable time constants.

TEA inhibition

Figure 2 shows examples of the action of TEA on current relaxations from −20 to −50 mV, and TEA inhibition curves, for the three currents studied.

Inhibition of currents generated by both tandem KCNQ3/2 and coexpressed KCNQ(2 + 3) constructs could be well-fitted by

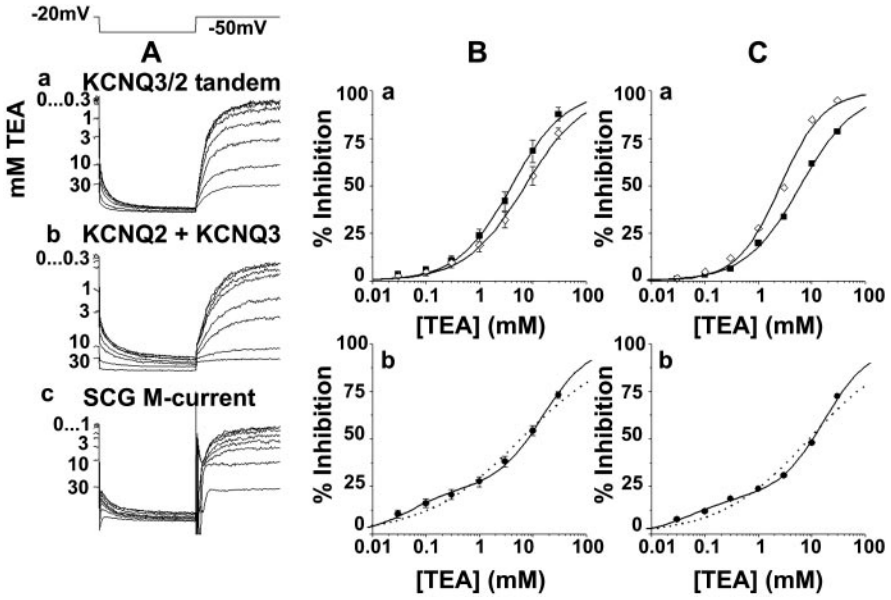

Figure 2. TEA inhibition of separately expressed and concatameric KCNQ2/3 currents are similar and in accord with a single-binding-site model, but two binding sites are required to fit M current inhibition curves in sympathetic neurons from P17 rats. *A*, Representative deactivation currents recorded on stepping for 1 sec from −20 to −50 mV (Fig. 1) in the presence of incremental concentrations of TEA (0.3–30 mM) for KCNQ3/2 tandem construct (*a*), coexpressed KCNQ2 and KCNQ3 constructs (*b*), and native M/KCNQ current (*c*) in P17 rat SCG neuron. *B*, Concentration dependence of inhibition of a KCNQ3/2 tandem (filled squares; $n = 11$) and cotransfected KCNQ2 plus KCNQ3 (open diamonds; $n = 12$) in CHO cells (*a*), and native M current (*b*) in SCG neurons ($n = 16–17$). Values plotted are means ± SE. Smooth lines superimposed on data sets are least-squares fits to unweighted data points, using one-component (dotted line) and two-component (solid line) Hill equations. Equation 1 is the basic equation. For the coexpressed KCNQ2 plus KCNQ3 constructs in *Ba*, $x_0 = 7.09 \pm 0.41$ mM and $p = 0.78 \pm 0.04$. For the tandem KCNQ3/2 construct in *Ba*, $x_0 = 3.97 \pm 0.23$ mM and $p = 0.86 \pm 0.04$. For the dotted curve in *Bb*, the constants were $x_0 = 5.95 \pm 0.32$ mM and $p = 0.48 \pm 0.046$. The two-component fit (*Bb*, solid line) is given by Equation 2, in which x_0 and x_1 are additionally the half-inhibitory concentrations (0.05 ± 0.013 and 15.15 ± 1.21 mM, respectively) for two channel types present in proportions q and $(1 - q)$, respectively, and $q = 0.24 \pm 0.016$. *C*, Concentration dependence fitted as in *B* but for single cells, exemplified by individual CHO cells expressing KCNQ3/2 tandem and KCNQ2 plus KCNQ3 (*a*) and an individual SCG neuron M-current (*b*) (symbols as in *B*).

a single-component Hill equation, with unity slopes [mean n_Hs ± SEM, 0.98 ± 0.08 for KCNQ3/2, and 0.97 ± 0.12 for KCNQ(2 + 3)], and overlapping IC_{50} values of 4.1 mM (95% CL, 2.4–6.9) for KCNQ3/2 and 6.7 mM (4.2–10.8) for KCNQ(2 + 3) (Fig. 2*Ba,Ca*). These IC_{50} values are in broad accord with previous measurements [3.5 mM for hKCNQ2 plus rKCNQ3 expressed in oocytes (Wang et al., 1998); 3.8 mM for hKCNQ2 plus rKCNQ3 in CHO cells: (Hadley et al., 2000); 10.5 mM for hKCNQ3/2 tandem (Wickenden et al., 2000)].

Single-component fits to the results obtained for inhibition of the native M current in 17 SCG neurons from P17 rats yielded an apparent geometric mean IC_{50} of 6.8 (3.7–8.5) mM; this was not significantly different from that for the inhibition of expressed KCNQ2 plus KCNQ3 or KCNQ3/2 channels. However, the mean of the individual slopes (0.56 ± 0.04) was significantly below unity, and a single-component fit to the mean data (Fig. 2*Bb*, dotted line) was relatively poor. This suggests that a uniform channel population was unlikely. Several (but not all) individual cells showed a noticeable biphasic inhibition, which was also apparent from the mean data (Fig. 2*Bb*). A two-component Hill equation gave an improved fit in most cases, as indicated both by visual matching to the data points and by the χ^2 value yielded during the least-squares fitting process. Inhibition data for 16 of 17 SCGs could be fitted satisfactorily with a two-component equation, and the fits from these 16 cells were used to derive a 95% confidence interval for the two resulting IC_{50}s. An initial attempt using previously obtained IC_{50} values (~0.3 and ~3 mM for KCNQ2 and KCNQ2 plus KCNQ3, respectively; Hadley et al., 2000) as fixed fitting parameters gave a poor fit. Allowing these parameters to float (with slopes constrained to unity) gave good fits: ~0.08 (0.05–0.13) and 16.4 (13.5–19.9) mM (Fig. 2*Bb,Cb*). The mean proportionate contribution of component 1 was 0.27 ± 0.03.

The range of IC_{50} values for the high-affinity component of TEA block (95% CL, 0.05–0.13 mM) overlaps with some of the values reported previously for the inhibition of homomeric KCNQ2 channels (means variably between 0.12 and 0.17 mM; Wang et al., 1998; Jow and Wang, 2000; Shapiro et al., 2000; Wickenden et al., 2000; Smith et al., 2001). Hence, this component might reflect a contribution by homomeric KCNQ2 channels to the total current. If so, this could relate to the age of the rats used (P17) because Tinel et al. (1998) have reported that KCNQ2 is expressed at an earlier developmental stage than KCNQ3 in mouse brain (see below). To test for this, we repeated the experiments on 10 SCG neurons isolated from 6-week-old rats (P45). In these experiments, the mean data were fitted equally well using a one- or two-component Hill equation (Fig. 3), and individual curves showed an improved fit using a two-component equation in only 2 of the 10 neurons. A one-component fit to each of the individual experiments yielded a geometric mean IC_{50} of 5.75 mM (95% CL, 3.1–10.7; i.e., within the range for inhibition of both KCNQ3/2 and KCNQ2 plus KCNQ3 currents), and a mean slope of 1.04 ± 0.13 (i.e., not significantly different from unity).

Single-cell PCR

To test further whether there might be a gross difference in the expression of KCNQ subunits between 17-d-old and 6-week-old rats, we performed single-cell PCR analyses of mRNAs for KCNQ2, 3, 4, and 5 in eight cells isolated from 17-d-old rats and seven cells isolated from 6-week-old rats (Fig. 4). All cells tested gave detectable signals for KCNQ2, 3, and 5; none gave a signal for KCNQ4.

Quantitative whole-ganglion PCR

The single-cell PCR experiments were not quantitative and so do not provide a measure of the relative amounts of different KCNQ mRNAs. To assess this, we made quantitative estimates of mRNA expression in whole ganglia isolated from rats at different developmental ages against GAPDH mRNA as an internal standard (Fig. 5). These yielded uniform levels of rKCNQ2 and rKCNQ5 mRNA throughout P7, P17, and P45, with negligible levels of rKCNQ4 mRNA. In contrast, rKCNQ3 mRNA increased progressively from a small excess at E18/E19 to a 10-fold excess at P45.

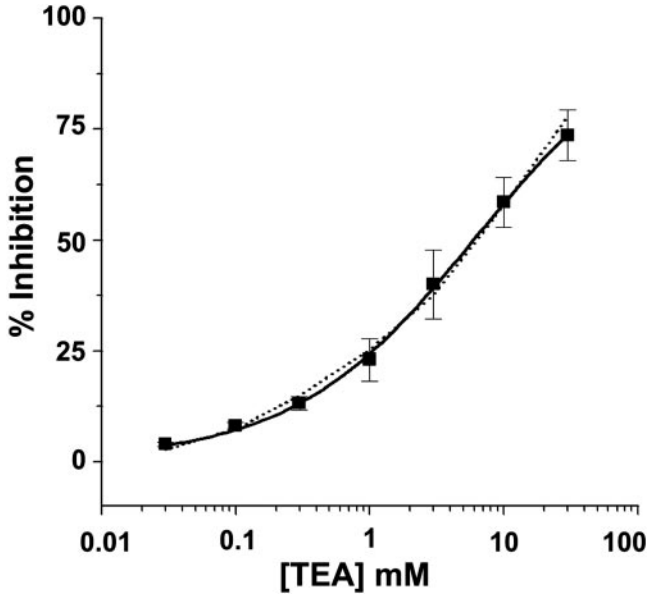

Figure 3. TEA inhibition of M currents in SCG neurons isolated from 6-week-old (P45) rats is in accord with a single-binding-site model. Each point shows the mean inhibition (± SEM) in 10 neurons, measured as described for Figure 2. The solid curve is a single-binding-site fit to Equation 1, with $x_0 = 6.0 \pm 0.3$ mM and $p = 0.63 \pm 0.02$. The interrupted line is a fit to the two-binding-site Equation 2, with $x_0 = 0.27 \pm 0.13$ mM, $x_1 = 12.3 \pm 3.8$ mM, and $q = 0.25 \pm 0.07$. The two-site model did not provide a significantly improved fit (compare Fig. 2*Bb*).

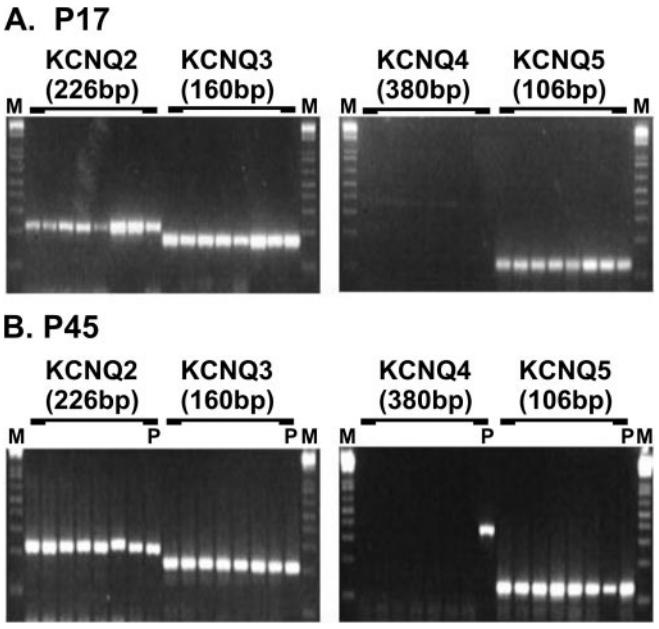

Figure 4. Single-cell PCR indicates the presence of mRNA for KCNQ2, KCNQ3, and KCNQ5, but not KCNQ4, in most SCG neurons tested at P17 and P45. Gels show bands from eight cells from P17 rats (*A*) and seven cells from P45 rats (*B*) using the primers described in Materials and Methods. Bands generated from the individual KCNQ cDNA plasmids are shown in the lanes marked P in *B*. No signals were detected in the absence of cDNA templates. M, Marker ladder.

Immunocytochemistry

Nearly all neurons showed substantial immunoreactivity for both KCNQ2 and KCNQ5 antibodies at both P17 and P45 stages (Fig. 6). In contrast, at P17, staining for KCNQ3 was relatively weak and irregular. However, at P45, most cells showed strong reactivity for KCNQ3, especially near the cell membrane. Staining for all

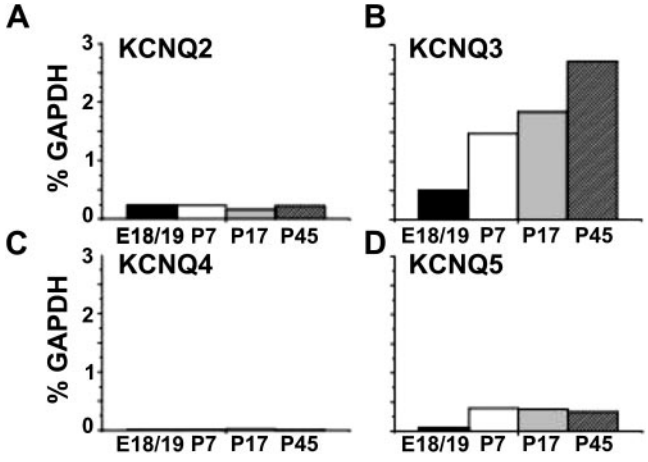

Figure 5. Quantitative RT-PCR analysis of KCNQ2 (*A*), KCNQ3 (*B*), KCNQ4 (*C*), and KCNQ5 (*D*) of whole ganglia isolated from rats at ages E18/E19 (black columns), P7 (white columns), P17 (gray columns), and P45 (hatched columns). KCNQ2–5 transcripts were normalized to GADPH levels and data were expressed as percent of GADPH.

three proteins was not confined to the soma, but extended along proximal processes. As a result, at P45, most cells stained for both KCNQ2 and KCNQ3, or for KCNQ5 and KCNQ3, when directly tested using double antibodies (Fig. 7). Because of the limited range of antibodies available, we could not directly show triple staining for KCNQ2, 3, and 5, but because very few cells were not stained by each of the antibodies, the majority of cells at P45 must have been immunoreactive for all three subunits.

Discussion

KCNQ expression in CHO cells

Currents generated by coexpressed KCNQ(2 + 3) cDNAs were virtually identical to those generated by the tandem KCNQ3/2 construct, in terms of both deactivation kinetics (Fig. 1) and TEA inhibition (Fig. 2).

As might be expected, inhibition of tandem KCNQ3/2 currents by TEA could be well fitted with a single-binding-site Hill equation with unity (0.98) slope. This slope value is the mean of the individual experiments. [In agreement with previous observations (Wickenden et al., 2000), the slope of the curve fitted to the mean data in Fig. 2*Ba* is less than unity; this is a consequence of the variation in IC_{50} values between different experiments, which ranged from 1.0 to 11.6 mM.] Assuming a single binding site to a tetrameric channel with a free energy of binding dependent on the number of tyrosines and threonines in the tetramer, and taking the binding constant for homomeric hKCNQ2 channels (with four tyrosines at position 284) to be 0.12–0.17 mM (see above), the predicted binding constant for hKCNQ3 (four threonines) would be between 100 and 140 mM. hKCNQ3 does not express well in CHO cells (Wickenden et al., 2000), but rKCNQ3 is clearly very insensitive to TEA, and this predicted value would be in accord with extrapolated values from previous (incomplete) concentration–inhibition curves (Hadley et al., 2000; Shapiro et al., 2000). These K_i values of ~0.15, 4.1, and ≥100 mM for KCNQ2, KCNQ3/2, and KCNQ3, respectively, are very close to those obtained by Liman et al. (1992) using tandem constructs containing different ratios (0–4) of wild-type and tyrosine-mutated Kv1.1 subunits. Thus, the data indicate that the tandem KCNQ3/2 construct assembles to yield a tetrameric channel with the pore formed from two KCNQ2 and two KCNQ3 subunits. [It has been reported previously that tandem *Shaker* constructs do not necessarily fix the stoichiometry of the ex-

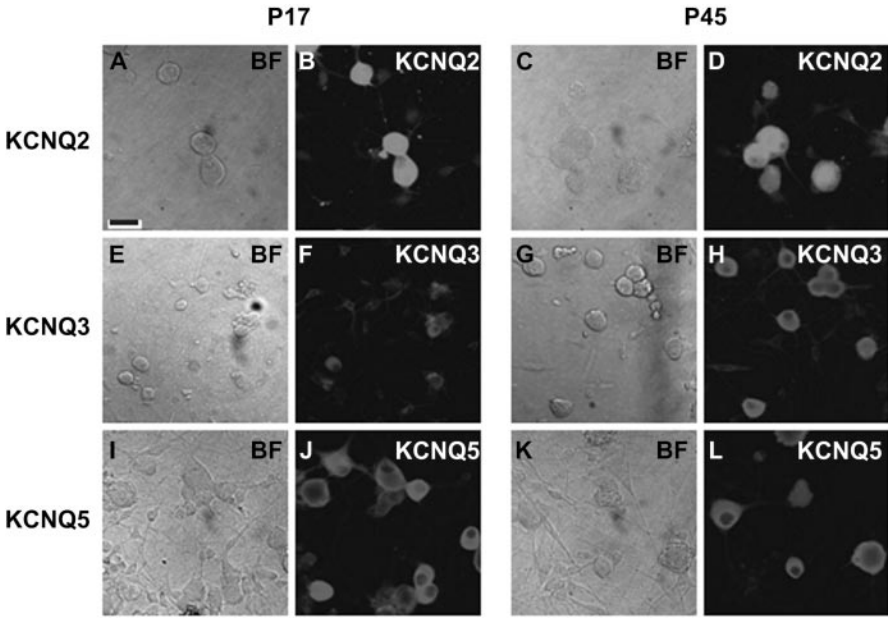

Figure 6. Immunocytochemical staining of P17 and P45 neurons with antibodies to KCNQ2, KCNQ3, and KCNQ5. The left panels of each pair show bright-field images; the right panels show corresponding dark-field fluorescence images. Note that nearly all neurons in the fields stained for KCNQ2 and KCNQ5 at both P17 and P45, and for KCNQ3 at P45, but that staining for KCNQ3 at P17 was sparser and weaker. Scale bar, 20 μm.

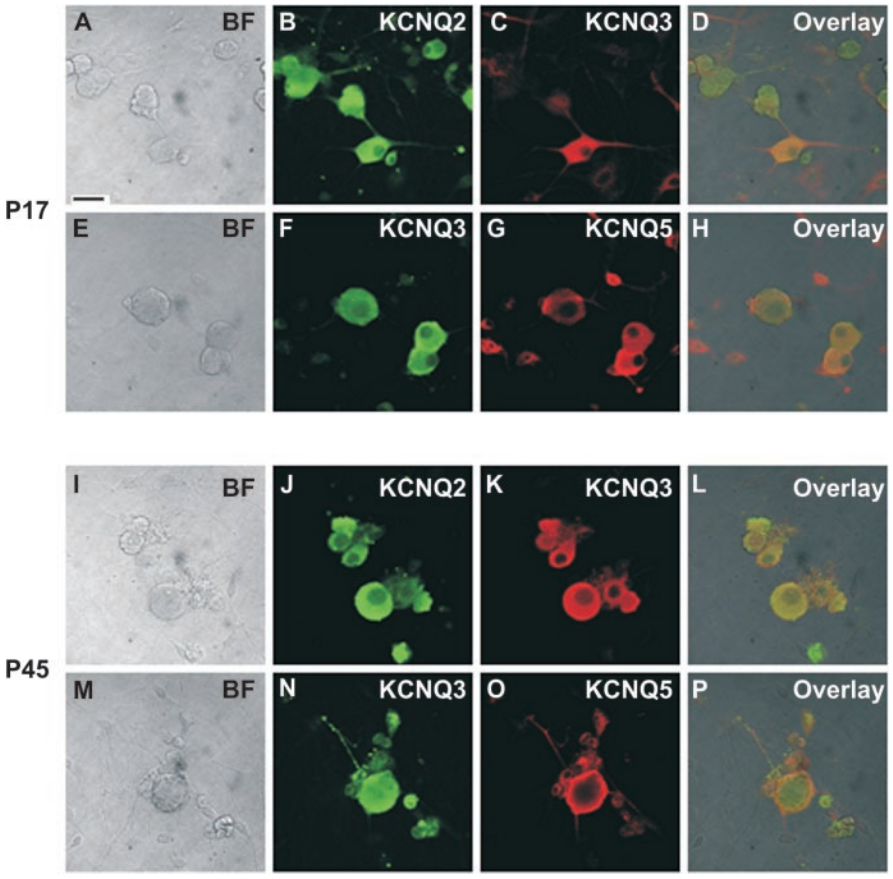

Figure 7. Double staining for KCNQ2 plus KCNQ3 (*A–D, I–L*) and KCNQ3 plus KCNQ5 (*E–H, M–P*) at P17 (*A–H*) and P45 (*I–P*). *A, E, I, M*, Bright-field images (BF). *D, H, L, P*, Electronic overlays of individual pictures. Note that, whereas most neurons show costaining for KCNQ2 and KCNQ3 at P45, many neurons in the field stain more strongly for KCNQ2 than for KCNQ3 at P17. Scale bar, 20 μm.

pressed channels after mRNA injection into oocytes, as judged by voltage-sensitivity (McCormack et al., 1992). However, other pharmacological studies on tandem *Shaker* constructs yielded data that accorded with the expected stoichiometry (Kavanaugh et al., 1992; Liman et al., 1992). Although a detailed kinetic comparison of homomeric KCNQ2 and KCNQ3 channels has not yet been completed, their voltage-sensitivity is too similar to allow accurate discrimination (Selyanko et al., 2000), but our pharmacological data clearly match that expected for a fixed stoichiometry.]

The results obtained using separate but coexpressed KCNQ2 and KCNQ3 cDNAs were indistinguishable from those obtained for the tandem construct. In particular, the unity Hill slope implies a single population of channels, and the intermediate IC_{50} accords with a 1:1 KCNQ2:KCNQ3 stoichiometry. Although it would be difficult to exclude entirely a contribution by homomeric channels (or by heteromeric channels with other stoichiometries) to the overall current, the number of such channels must be very small because the conductances and open probabilities of individual homomeric KCNQ2 or KCNQ3 channels do not differ substantially from those of the heteromeric (coexpressed) channels when expressed in CHO cells (Selyanko et al., 2001). Thus, our data do not support a random assembly of subunits (cf. Shapiro et al., 2000). Perhaps, as suggested for Kv1.3 channels (Tu and Deutsch, 1999), channel assembly proceeds through the formation and subsequent association of KCNQ3/2 subunit dimers. Because the surface expression of both KCNQ2 and KCNQ3 subunits is greatly enhanced by heteromeric expression (Schwake et al., 2000), heteromeric KCNQ3/2 dimer formation followed by dimer–dimer assembly seems most likely.

Native M channels

Although the data for SCG neurons was somewhat more variable, results obtained using ganglion cells isolated from 6-week-old (P45) rats were statistically indistinguishable from those obtained for expressed KCNQ3/2 and KCNQ2 plus KCNQ3 channels (geometric mean IC_{50}, 5.75 mM; mean Hill slope, 1.04). Hence, it seems reasonable to presume that native KCNQ/M currents in these cells are also carried predominantly by channels with the same stoichiometry (2×KCNQ2 plus 2×KCNQ3).

In contrast, many neurons isolated from 17-d-old (P17) rats showed a clear biphasic concentration–inhibition curve,

as did the mean curve. This curve did not accord with random assembly, but instead could be better fitted by assuming two populations of channels with differing affinities for TEA. One possibility is that currents were contaminated by current flow through other, more sensitive, K^+ channels but this seems unlikely because the kinetics of the deactivation tails (from which inhibition was calculated) accorded with those for expressed KCNQ channels. Instead, the data could be interpreted by assuming that, in these younger neurons, some 26% (on average) of the current was carried by homomeric KCNQ2 channels.

This probably results from a developmental delay in KCNQ3 expression. Thus, the quantitative PCR data showed incrementing levels of KCNQ3 mRNA at P7, P17, and P45, whereas levels of KCNQ2 and KCNQ5 mRNA remained approximately constant over this developmental period. This accords with previous reports that KCNQ2 mRNA expression reaches the adult level by P7 in mouse brain, whereas KCNQ3 mRNA is very low at P3 and continues to increase up to P30 (Tinel et al., 1998). Likewise, at P17, immunohistochemical staining for KCNQ3 protein was relatively sparse, such that many neurons were devoid of clear staining, whereas nearly all stained for KCNQ2; by P45, nearly all neurons showed strong staining for KCNQ3 protein, particularly at or near the cell membrane. It might be suggested that the excess message for KCNQ3 revealed by the quantitative PCR serves to ensure the appropriate formation and membrane insertion of heteromeric KCNQ2/3 channels.

Another cause of variability in both the kinetics and TEA sensitivity of ganglion cell currents might be the variable expression of different C-terminal splice variants of KCNQ2 (Pan et al., 2001; Smith et al., 2001). Thus, exon 15a in rat KCNQ2, which slows deactivation kinetics (Pan et al., 2001), is not present in the human KCNQ2 sequence; this might account for the slightly faster deactivation kinetics of expressed hKCNQ3/2 tandem constructs and coexpressed hKCNQ plus rKCNQ3 constructs (time constants, 60 and 220 msec, and 58 and 280 msec, respectively) than those of native rat ganglion cell M currents (time constants 70 and 280 msec at −50 mV). It has also been reported that a C-terminal-truncated splice variant of KCNQ2 (Q2S) (Tinel et al., 1998) is expressed in human fetal (but not adult) brain; this does not generate currents of itself but, when coexpressed with the normal long form (Q2L), reduced current density and (rather surprisingly) appeared to increase sensitivity to TEA (Smith et al., 2001). If expressed in immature rat neurons this might affect our measurements of TEA inhibition.

KCNQ5?

In confirmation of previous *in situ* hybridization results (Schroeder et al., 2000), PCR analysis revealed mRNA levels for KCNQ5 at least as great as those for KCNQ2. Furthermore, single-cell PCR indicated coexpression of KCNQ2, 3, and 5 mRNA in all individual cells tested. Coexpression of KCNQ2 and 5 protein (and, at P45, KCNQ3 protein) in most neurons can also be inferred from the immunohistochemical data. This raised the question: To what extent do currents through heteromeric KCNQ3/5 channels (and/or homomeric KCNQ5 channels) contribute to the macroscopic currents recorded from these neurons?

KCNQ5 currents are much more insensitive to TEA than KCNQ2 currents (IC_{50} 71 mM; Schroeder et al., 2000), so a KCNQ3/5 heteromultimer would be predicted to have an IC_{50} of ~100 mM. This is well above the maximum concentration (30 mM) used in the present experiments. Thus, a contribution of KCNQ3/5 channels to the current would be identifiable only by an extrapolated submaximal inhibition predicted from the single-site KCNQ3/2 inhibition curve. In the 6-week-old neurons, unconstrained concentration–inhibition curves extrapolated to a mean maximum inhibition of 93.7 ± 7.1%. Thus, the contribution of KCNQ3/5 to the native ganglionic M current is likely to be small. However, this may be variable because in 3 of 10 cells the inhibition curves attained a clear, observable maximum between 70 and 80% inhibition above 3–10 mM TEA. In this regard, sympathetic neuron M currents resemble those in hippocampal pyramidal cells where (in spite of clear coexpression of KCNQ2 and KCNQ5 mRNA and protein) in terms of TEA block, the majority of cells behaved as if KCNQ2/3 channels carried all of the somatic M current, with only a minority (30%) showing incomplete block, implying a contribution by KCNQ5 subunits (Shah et al., 2002).

One possible explanation for the relative paucity of KCNQ3/5 (or KCNQ5) currents might be that these channels have a very much lower conductance than KCNQ2/3 channels. However, this appears not to be the case. KCNQ3/5 heteromultimers, either coexpressed (Lerche et al., 2000; Schroeder et al., 2000) or expressed as tandem constructs, generate substantial currents (Wickenden et al., 2001). Furthermore, preliminary experiments using KCNQ3/5 tandem constructs expressed in CHO cells suggest a single-channel conductance of ~3–4 pS in asymmetric potassium (estimated from single-channel currents recorded at potentials between −10 and 0 mV: G. Passmore, unpublished observations): approximately half of that (~8 pS) of KCNQ(2 + 3) channels (Selyanko et al., 2001) or of concatameric KNCQ3/2 channels (~8–10 pS: G. Passmore, unpublished observations) when measured at depolarized potentials.

Irrespective of the reason for the apparently weak contribution of KCNQ5 subunit channels to the macroscopic ganglion cell currents, the present results are in accord with previous inferences (Wang et al., 1998; Shapiro et al., 2000; Selyanko et al., 2001) that the native M current in mature rat ganglion cells is carried predominantly by KCNQ2/3 heteromultimers, and also indicate that these two subunits coassemble in equal stoichiometric proportions. They also suggest that the formation of the mature heteromeric channel is developmentally regulated, probably through progressively increasing expression of the KCNQ3 subunit.

References

Brown DA (1988) M currents. In: Ion channels (Narahashi T, ed) Vol 1, pp 55–99. New York: Plenum.

Brown DA, Adams PR (1980) Muscarinic suppression of a novel voltage-sensitive K^+ current in a vertebrate neuron. Nature 283:673–676.

Christie MJ, North RA, Osbourne PB, Douglas J, Adelman JP (1990) Heteropolymeric potassium channels expressed in *Xenopus* oocytes from cloned subunits. Neuron 2:405–411.

Cooper EC, Aldape KD, Abosch A, Barbaro NM, Berger MS, Peacock WS, Jan YN, Jan LY (2000) Colocalization and coassembly of two human brain M-type potassium channel subunits that are mutated in epilepsy. Proc Natl Acad Sci USA 97:4914–4919.

Gibson UE, Heid CA, Williams PM (1996) A novel method for real time quantitative RT-PCR. Genome Res 6:995–1001.

Hadley JK, Noda M, Selyanko AA, Wood IC, Abogadie FC, Brown DA (2000) Differential tetraethylammonium sensitivity of KCNQ1–4 potassium channels. Br J Pharmacol 129:413–415.

Heginbotham L, MacKinnon R (1992) The aromatic binding site for tetraethylammonium ion on potassium channels. Neuron 8:483–491.

Heid CA, Steven J, Livak KJ, Williams PM (1996) Real time quantitative PCR. Genome Res 6:986–944.

Jentsch TJ (2000) Neuronal KCNQ potassium channels: physiology and role in disease. Nat Rev Neurosci 1:21–30.

Jow F, Wang K (2000) Cloning and functional expression of rKCNQ2 K^+ channel from rat brain. Brain Res Mol Brain Res 80:269–278.

Kavanaugh MP, Varnum MD, Osborne PB, Christie MJ, Busch AE, Adelman JP, North RA (1991) Interaction between tetraethylammonium and amino acid residues in the pore of cloned voltage-dependent potassium channels. J Biol Chem 266:7583–7587.

Kavanaugh MP, Hurst RS, Yakel J, Varnum MD, Adelman JP, North RA (1992) Multiple subunits of a voltage-dependent potassium channel contribute to the binding site for tetraethylammonium. Neuron 8:493–497.

Lamas JA (1998) A hyperpolarization-activated cation current (I_h) contributes to resting membrane potential in rat superior cervical ganglion neurones. Pflügers Arch 436:429–435.

Lerche C, Schere CR, Seebohm G, Derst C, Wei AD, Busch AE, Steinmeyer K (2000) Molecular cloning and functional expression of KCNQ5, a potassium channel subunit that may contribute to neuronal M-current diversity. J Biol Chem 275:22395–224000.

Liman LR, Tytgat J, Hess P (1992) Subunit stoichiometry of a mammalian K^+ channel determined by construction of multimeric cDNAs. Neuron 9:861–871.

MacKinnon R, Yellen G (1990) Mutations affecting TEA blockade and ion permeation in voltage-activated K^+ channels. Science 250:276–279.

Marrion NV (1997) Control of M-current. Annu Rev Physiol 59:483–504.

McCormack K, Lin L, Iversen LE, Tanouye MA, Sigworth KJ (1992) Tandem linkage of Shaker K^+ channel subunits does not ensure the stoichiometry of expressed channels. Biophys J 63:1406–1411.

Owen DG, Marsh SJ, Brown DA (1990) M-current noise and putative M-channels in cultured rat sympathetic ganglion cells. J Physiol (Lond) 431:269–290.

Pan Z, Selyanko AA, Hadley JK, Brown DA, Dixon JE, McKinnon D (2001) Alternative splicing of KCNQ2 potassium channel transcripts contributes to the functional diversity of M-currents. J Physiol (Lond) 531:347–358.

Rae J, Cooper K, Gates P, Watsky M (1991) Low access resistance perforated patch recordings using amphotericin B. J Neurosci Methods 37:15–26.

Schroeder BC, Hechenberger M, Weinreich F, Kubisch C, Jentsch TJ (2000) KCNQ5, a novel potassium channel broadly expressed in brain, mediates M-type currents. J Biol Chem 275:24089–24095.

Schwake M, Pusch M, Kharkovets T, Jentsch TJ (2000) Surface expression and single channel properties of KCNQ2/KCNQ3, M-type K^+ channels involved in epilepsy. J Biol Chem 275:13343–13348.

Selyanko AA, Hadley JK, Wood IC, Abogadie FC, Delmas P, Buckley NJ, London B, Brown DA (1999) Two types of K^+ channel subunit, Erg1 and KCNQ2/3, contribute to the M-like current in a mammalian neuronal cell. J Neurosci 19:7742–7756.

Selyanko AA, Hadley JK, Wood IC, Abogadie FC, Jentsch TJ, Brown DA (2000) Inhibition of KCNQ1–4 potassium channels expressed in mammalian cells via M_1 muscarinic acetylcholine receptors. J Physiol (Lond) 522:349–355.

Selyanko AA, Hadley JK, Brown DA (2001) Properties of single M-type KCNQ2/KCNQ3 potassium channels expressed in mammalian cells. J Physiol (Lond) 534:15–24.

Shah MM, Mistry M, Marsh SJ, Brown DA, Delmas P (2002) Molecular correlates of the M-current in cultured rat hippocampal neurons. J Physiol (Lond) 544:29–37.

Shapiro MS, Roche JP, Kaftan EJ, Cruzblanca H, Mackie K, Hille B (2000) Reconstitution of muscarinic modulation of the KCNQ2/KCNQ3 K^+ channels that underlie the neuronal M-current. J Neurosci 20:1710–1721.

Smith JS, Iannotti CA, Dargis P, Christian EP, Aiyar J (2001) Differential expression of KCNQ2 splice variants: implications to M-current function during neuronal development. J Neurosci 21:1096–1103.

Tinel N, Lauritzen I, Chouabe C, Lazdunski M, Borsotto M (1998) The KCNQ2 potassium channel: splice variants, functional and developmental expression: brain localization and comparison with KCNQ3. FEBS Lett 438:171–176.

Tu L, Deutsch C (1999) Evidence for dimerization of dimers in K^+ channel assembly. Biophys J 76:2004–2017.

Wang HS, Pan Z, Shi W, Brown BS, Wymore RS, Cohen IS, Dixon JE, McKinnon D (1998) KCNQ2 and KCNQ3 potassium channel subunits: molecular correlates of the M-channel. Science 282:1890–1893.

Wickenden AD, Yu W, Zou A, Jegla T, Waggoner PK (2000) Retigabine, a novel anticonvulsant, enhances activation of KCNQ2/3 potassium channels. Mol Pharmacol 58:591–600.

Wickenden AD, Zou A, Wagoner PK, Jegla T (2001) Characterization of KCNQ5/3 potassium channels expressed in mammalian cells. Br J Pharmacol 132:381–384.

Yang WP, Levesque PC, Little WA, Conder ML, Ramakrishnan P, Neubauer MG, Blanar MA (1998) Functional expression of two KvLQT1-related potassium channels responsible for an inherited idiopathic epilepsy. J Biol Chem 273:19419–19423.

Zawar C, Plant TD, Schirra C, Konnerth A, Neumcke B (1999) Cell-type specific expression of ATP-sensitive potassium channels in the rat hippocampus. J Physiol (Lond) 514:327–341.